Lasers in Manufacturing Conference 2023

Decreasing feature size of surface texturing structures created by laser dispersing of ceramic particles.

B.R. Ettema[a,*], G.R.B.E. Römer[a], D.T.A. Matthews[b]

[a]*Chair of Laser Processing,* [b]*Functional Surface Engineering & Design, Department of Mechanics of Solids, Surface & Systems (MS³), Faculty of Engineering Technology, University of Twente, Drienerloolaan 5, Enschede 7522 NB, The Netherlans*

Abstract

Wear resistance of the surface of steel rolls, used to transfer desired roughness profiles onto steel strip in steel production, can be improved by embedding micrometer sized ceramic particles from a preplaced layer into a tool steel surface utilizing locally derived laser-induced melt pools, in a process termed laser implantation. Dome shaped surface structures with significantly increased hardness can be achieved. Reported experiments in literate focus on implantations with 150-400 µm diameter and 10-30µm in height. However, features with smaller diameter and height are desired for technology adoption. This paper presents and discusses first experimental results of implantations with a diameter below 150 µm, with heights between 1-15 µm and significantly increased hardness. For that purpose, a Nd:YAG laser source (focal diameter 54 µm, pulse times t_p= 3-15 ms, pulse power 20-50 W average) was used to induce a melt pool driving the embedding.

Keywords: laser implantation; laser dispersion; ceramic particles; surface texturing

1. Introduction

Large quantities of surface textured sheet metal is commonly produced using skin pass rolling. In this technique, the skin pass roll acts as a die, embossing the surface texture on the roll into the sheet metal. However, the surface texture on the sheet metal is limited by the production method of the negative surface texture on the skin pass roll. Furthermore, the production cost and product quality of the sheet texture is effected by the degradation rate of the skin pass roll texture during a rolling campaign. Currently most used

* Corresponding author
E-mail address: b.r.ettema@utwente.nl.

roll texturing methods, such as shot blasting and Electrical Discharge Texturing (EDT) (Morgan, 1996) either remove or displace the base material in/of the surface of the skin pass roll. These methods result in stochastic surface textures on the roll. Furthermore, commonly, hard chrome plating is applied that improve the wear resistance (Kleinz, 1992). However, because of its toxicity, chrome is banned from industrial applications (Gaspard, 2016). Last, but not least, additional deterministic design freedom is required in terms of the surface texture design on the roll and correspondingly on the steel strip, which can obviously not be offered by stochastic texturing methods, mentioned above. Gorbunov et al. compared five texturing techniques, which allow to create (pseudo-)deterministic textures on the skin pass rolls, but rely on either micrometric subtractive techniques or on the displacement of material on the micro meter scale on the roll. Instead, of material removal (subtraction) or displacement an additive material technique, to create a surface texture, has the potential to offer a laser design freedom for deterministic textures, as well as improve the wear resistance of the texture, and therefore also of the roll.

An additive technique known as “laser implantation texturing” (Hilgenberg and Steinhoff, 2015), coined here as “LITex", allows to deposit a deterministic texture, consisting of a pattern of “implants”, on a substrate. This process is also known as laser dispersing (Hilgenberg, 2014). By careful selection of the added material the local hardness of the texture can be increase, potentially eliminating the need for chrome plating. Laser implantation texturing (LITex) consist of three steps as schematically shown in Fig. 1. In the first step a thin layer (typically 100 µm and thicker), consisting of a paste of small hard particles in a binder (e.g. Polyvinylbutyral (PVB)), which is applied on top of the substrate using a mask and a knife edge. The typically ceramic particles are hard and have a melt temperature (much) higher than the melt temperature of the substrate. In the second step, the powder layer is irradiated by a pulsed laser beam, during which the binder evaporates, the substrate melt and the particles submerge, unmolten, in the melt pool. After the laser pulse, the hard particles are embedded in the resolidified melt pool, forming a “hump” (implant). In the third step, the excess of paste around the implant is removed in a cleaning step. The implantation process is repeated by moving the laser beam or the substrate to a next location, to form patterns of implants.

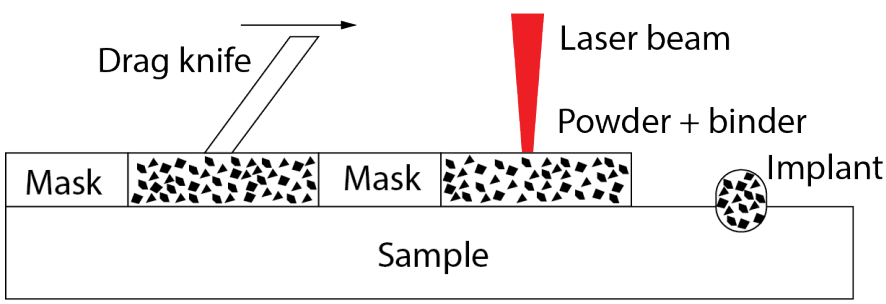

Fig. 1. Schematic representation of the various steps in the laser implantation process. Left: application of a powder layer (powder particles in a binder) using a knife edge and a mask. Center: laser-induced implantation of the particles. Right: removal of excess powder (cleaning) around the implant.

In this approach, Spranger and Hilgenberg (2019) achieved implantation diameters ranging from 150µm to 350 µm and heights ranging from 10µm to 30 µm heights, using pulse powers of 40 W to 180 W, laser focal diameter of 105 µm, pulse duration of 3-15 ms and a powder layer thickness of 100 µm consisting of TiB2 particles ranging between 5 µm and 13 µm. They reported a hardness up to 1800 Hv of the texture on a AISI D2 substrate. However, for industrial application in skin rolls, requiring a deterministic pattern, smaller

implantation diameters, of less than 150 µm are needed The work presented in this paper presents and discusses our efforts to achieve smaller implantation diameter while still maintaining the hardness increase offered by the ceramic particles. To that end, the processing window for laser processing parameters, including, but not limited to, the layer thickness and spots size, is established experimentally.

2. Methodologies

2.1. Experimental setup

Fig. 2a shows a schematic of the experimental setup. It hosts YAG laser source (JK100FL of JK Lasers, UK)which emits a beam with a Gaussian intensity profile (M^2=1.23) at wavelength of 1080 nm. The beam is transported through an optical fiber to a collimator with focal length of 76 mm A dichroic mirror deflects the laser radiation, but is transparent for light in the visible spectrum originating from the laser material interaction zone on the substrate. The latter would allow in-situ camera imaging. Two 1:1 beam splitters (Thorlabs CCM1- BS014/M) are used to reduce the laser power to levels needed during the LITex process, while being able to run the laser source reliably at high laser power levels. After the beam splitters, the laser beam is focussed to a diameter of 54 µm, using a lens (JK Lasers, UK) with a focal length of 300 mm. One of the outputs of the second beam splitter is directed to a high speed laser power sensor (BM-A-5W-14-T of Laser point, Italy) to verify the pulse durations of the laser pulse. Close to the surface of the substrate a flow (10 l/min) of argon is supplied through a nozzle, to prevent the laser-material interaction from oxidation. Fig. 2b shows a pictures of the experimental setup used.

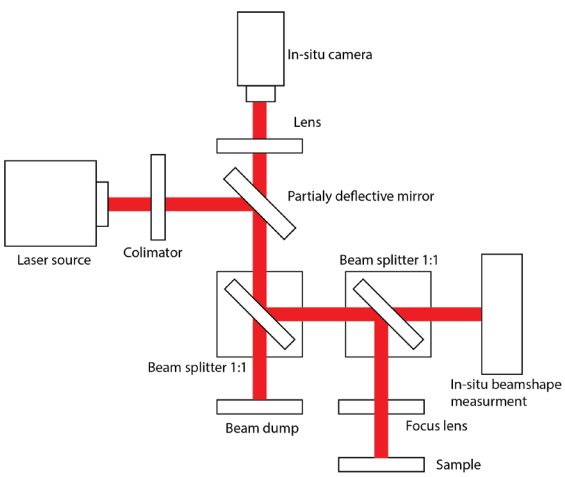

(a) Schematic overview laser setup Beam line

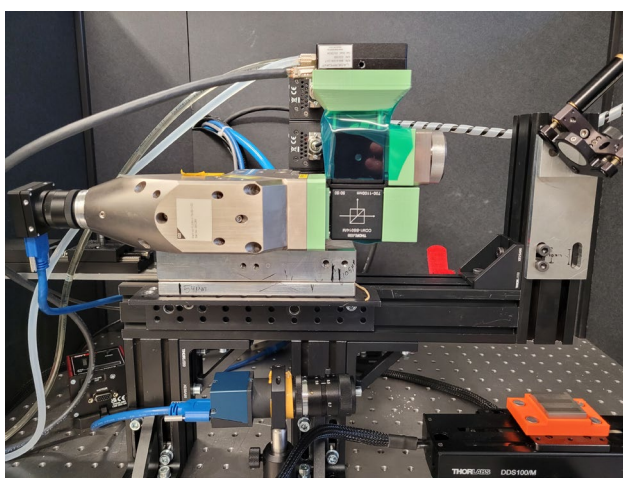

(b) Picture of laser setup

Fig. 2. Experimental laser setup.

2.2. Materials

The substrate consist of 30 × 30 mm^2 slabs of X100CrMoV5 tool steel (see Table 1) with a thickness of 6 mm. This tool steel is frequently used for skin pass rolls. The chromium carbides in this ledeburitic steel results in high wear resistance and high ductility The surface of the samples were polished to a roughness of R_a=0.2 µm. Next, is the samples were hardened and annealed, resulting in a hardness of 600 Hv, which is typical for skin-pass rolls. The melting point and density of the material are listed also in Table 1.

The particles to be implanted shall have a high hardness than the substrate, as well as a higher melting point than the tool steel (substrate). This will result in reduced wear of the skin roll surface, compared to a bare steel surface without the implants. In addition, the particles should shall show a low thermal expansion coefficient to avoid stress during solidification. Therefore Tungsten Carbide (WC) particles were chosen. The diameter of the particles shall be significantly smaller than the target diameter of the implant. Therefore WC with mean diameters smaller than 2 µm, supplied by Sigma-Aaldrich were chosen Polyvinyl butyral (PVB) with ethanol solvent is used as binder to form a paste (94% WC particles and 6% PVB mass) which can be applied in layer of uniform thickness on the substrate. To that end paste is spread on a mask and dragged over the sample using a knife edge. A mask with a thickness of 50 µm was used to create a powder layer of 50 µm. The maximum variation in the layer was found to be 5 µm.

Table 1. Material properties

Material	Density	Melt temperature	Hardness	Ra
X100CrM0V5	7750 kg/m3	1421 °C	600 Hv	0.2 µm
WC < 2 µm	4520 kg/m3	3230 °C	2600 Hv	
PVB	1080 kg/m3	165 °C	n.a.	

2.3. Analysis tools

A Scanning Electron Microscope (JSM-7200F, JEOL, Japan) is employed to assess geometrical features of the implants. Using this SEM, EDX imaging (Oxford instruments, UK) is preformed to identify the location and concentration of WC in the implants. Micro hardness measurements over surface of the implants using a Anton Paar NHT2 nano indenter. The hardness values of eight measurements spaced evenly over the implant diameter are averaged. The dimensions (diameter and average height) of the implants are obtained using confocal microscopy (S NEox, Sensofar, Spain) The diameter of a (in some cases) elliptical shaped implant is calculated form the confocal data as the average length of the long and short axis of the implant. Similarly the height of an implant is calculated from the average of the maximum height along the long axis and the maximum height along the short axis of the implant.

2.4. Methodologies

In this work the laser power during the laser pulse is set to a value ranging from 20 to 50 W, see Table 2. The laser pulse duration was set to values ranging from 3 ms to 15 ms are used. For each combination of laser power and pulse duration 9 experiments were performed, to assess the statistical reliability of the implantation process. That is, for each combination of laser power and pulse duration the average dimensions and standard deviations of the implants were determined based on 9 experiments.

Table 2. Experimental parameters

Parameter	Value(s)
Laser wavelength	1080 nm
Spot size	54 µm
Density of WC powder layer	94%
Powder layer height	50 ± 5 µm
Pulse durations	3, 6, 9, 12, 15 ms
Range of laser powers during the pulse (on the powder layer)	20, 30, 40, 50 W

3. Results and discussion

3.1. Increased hardness

Fig. 3a shows a SEM micrograph of an exemplary single implant, after the cleaning step. In this figure the (size of the) laser spot diameter is visualized by a red dotted circle . In this SEM micrograph the implant shows a diameter larger than the laser spot diameter, characterized by the light gray perimeter outside the laser spot. Hence, it can be concluded that the diameter of the melt pool during the implantation process is larger than the diameter of the laser spot. The black region around it is the unaffected bare substrate surface. Fig 3b. shows the EDX analysis of the same implant , clearly showing the presence of WC particles in the implant. Also from this analysis it can be concluded the diameter melt pool was larger than the diameter of the laser spot. The EDX image suggests that WC is only found in the perimeter of the implant, and not or at least a reduced concentration in the center of the implant. However, it can be argued that temperature induced variations in the surface tension coefficient surface of the melt pool induce fluid flows (Marangoni) flows which drive WC particles down into the melt pool. As a result, WC particles might be found, at a high(er) concentration, just below the surface of the implant, additional research needs to confirm this.

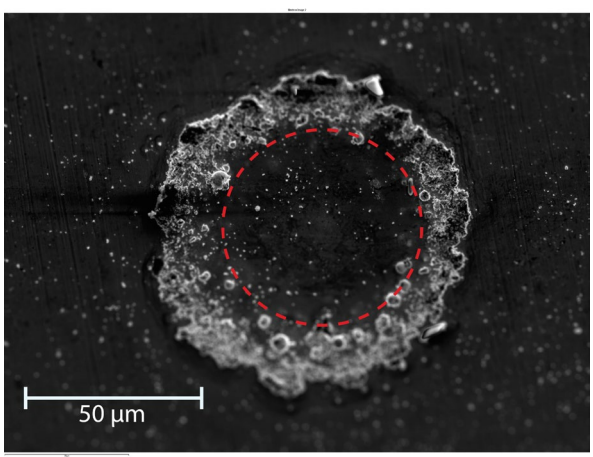

(a) SEM micrograph. The dotted circle marks the diameter of the laser spot.

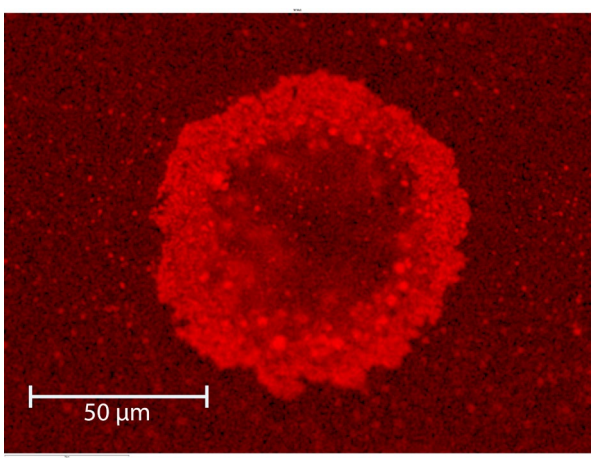

(b) EDX image of the implant showing (in red) the tungsten content [a.u.].

Fig. 3. SEM and EDX image of an implant created at a pulse duration of 9 ms at a pulse power of 30 W

Before implantation , the hardness of the bare substrate was measured and found to equal 660 Hv, see table 2. Next, the hardness of the laser-material interaction zone of remelting of the substrate was measured. That is, the bare surface, without a powder layer, was melted by exposing it to a laser pulse of 20 W and 9 ms pulse duration. The average hardness of the resulting laser-material interaction zone was found to equal 720 Hv, which is harder than the hardness of the as received substrate. Last, but not least, the average hardness of the implants is 1154 Hv. The latter is similar to the hardness values reported by Hilgenberg and Steinhof (2015).

Table 2. Results of hardness measurements (averaged values)

Material	Hardness
Base material	600 Hv
Laser melted (no powder)	720 Hv
Implantation with WC	1154 Hv

3.2. Dimensions of implants

Fig. 4 shows the averaged diameters and height of implants as function of the laser power in the pulse. As can be observed from Fig. 4a the implantation diameter decreases with decreasing laser pulse power. It can also be concluded from this graph that decreasing the pulse duration decreases the implant diameter. The latter can be attributed to lower the fluence the melt pool is subjected to. All in all, it can be concluded from this graph that significantly smaller implant diameters, than reported in literature, can be reliably achieved, provided that the layer thickness (here 50 µm) is chosen smaller than typically applied (100 µm) in literature Hilgenberg and Steinhof (2015). Similarity, the average height of the implants (Fig. 4b) also shows a decreasing trend, when decreasing the laser power in the pulse. However, the spread in the height values are higher than the spread in the diameter of the implant, especially for a pulse duration of 15 ms. For laser pulse powers of 30 W and less, the spread in the height of the implants for all pulse durations is small(er). Furthermore, the difference in height between the 3 and 6 ms pulse time is more significant than that between 6 ms and 12 ms pulse time. It can also be concluded from this graph that decreasing the pulse duration decreases the implant height. The latter can be attributed higher temperatures in the melt pool increasing the viscosity and decreasing the surface tension. It is noteworthy that the height of implants achieved at a pulse duration of 6 ms and a pulse power of 40 W is close to the height found in literature (Hilgenberg and Steinhof 2015), whereas at this parameter combination, the diameter of the implant (Fig,. 4a) is smaller than the diameters found in literature. Hence, by reducing the laser pulse power, powder layer thickness and pulse duration, not only smaller implants can be achieved, but also implants with a high aspect ratio.

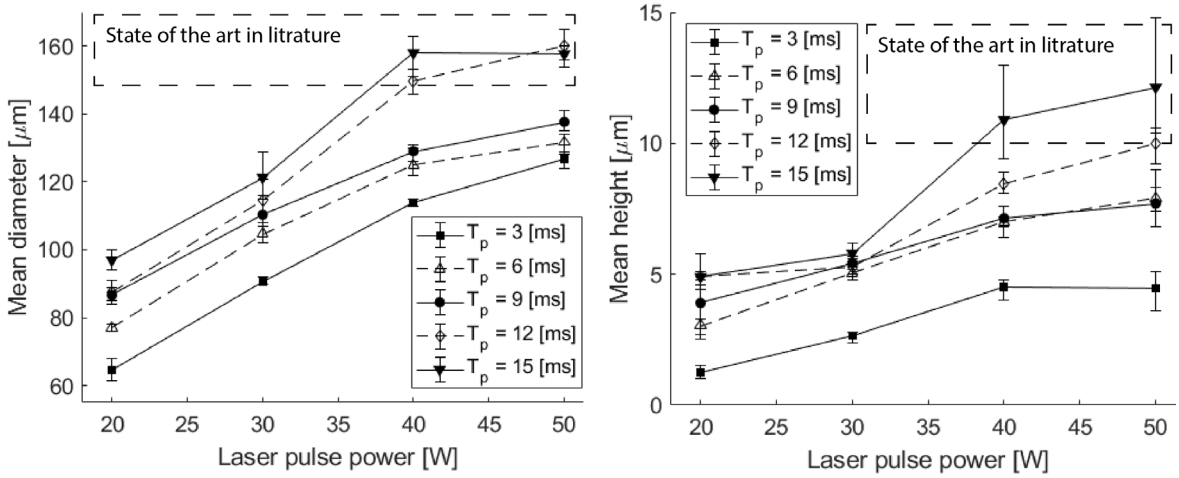

(a) Diameter of implant as function of laser pulse power.

(b) Height of implant as function of laser pulse power.

Fig. 4. Dimensions of implants as function of the laser pulse power and pulse duration T_p, layer height 50 µm, powder density 94% (WC particles < 2µm) and laser spot diameter of 54 µm

4. Conclusions and outlook

Experimental results of Laser Implantation Texturing (LITex), aka laser dispersing, using tungsten carbide particles (<2 µm) in a 50 µm powder layer on a tool steel substrate, using a YAG laser (pulse power 20 W to 50 W, pulse duration, 3 ms to 15 ms, spot size 50 µm) were analyzed. Implant diameters ranging from 64 µm to 159 µm, and implant heights ranging from 1 µm to 13 µm were found. Also, it was found that decreasing the laser pulse power decreases the dimensions of the implants. Additionally, increasing the laser pulse time increases the dimensions of the implants. An implantation diameter as small as 64 µm and heights as small as 1 µm can be reliably achieved. However, the stability of the LITex process reduces if laser pulse powers of more than 30 W are applied. The found diameters of implants obtained at less than 30 W, are smaller than implant dimensions than reported in literature. These smaller dimensions are essential for the applicability of LITex as a laser patterning technique in texturing of skin pass rolls in steel industry. Micro-hardness measurements of the implants show an average hardness of 1152HV, which is well above the hardness of 600 HV of the virgin tool steel substrate. The higher hardness of the implants will contribute to the wear resistance of the surface.

Future work will include similar LITex experiments to further optimize the laser parameters (process window), as well as using other (different) ceramic particles. In addition, tribological wear testing, simulating cold rolling contact conditions, are planned to characterize the wear process and wear resistance of surfaces with implants.

Acknowledgements

The project has received funding through the Top consortium for Knowledge and Innovation (TKI) program of the Dutch ministry of Economic Affairs, as well as from, and collaboration n with Tata Steel Nederland Technology B.V.

References

L.A. Dobrzański, K. Labisz, E. Jonda, A. Klimpel, 2007. Comparison of the surface alloying of the 32CrMoV12-28 tool steel using TiC and WC powder, Journal of Materials Processing Technology, Volume 191, Issues 1–3, Pages 321-325.

C. Gaspard,H. Bolt, J. Bertrandie, 2016. European Commission, Directorate-General for Research and Innovation, European Commission, Directorate-General for Research and Innovation Substitution of chrome plating for the rolls of skin-pass mill (CRFREEROLLS) – Final report, Publications Office.

A. V. Gorbunov, V. K. Belov and D. O. Begletsov, 2009. Texturing of rollers for the production of auto-industry sheet. *Steel in Translation* 39, 696.

K. Hilgenberg, K. Steinhoff, 2015. Texturing of skin-pass rolls by pulsed laser dispersing. *Journal of Materials Processing Technology* 225, 84 – 92.

K. Hilgenberg, K. Behler, K. Steinhoff, 2014. Localized dispersing of ceramic particles in tool steel surfaces by pulsed laser radiation, Applied Surface Science, Volume 305, Pages 575-580.

H. Kleinz, H.U., 1992. Hard-chromed work rolls for the production of cold-rolled sheet. *Metallurgical Plant Tech* 6, 76–82.

P. Kron, 1996. Verschleissschutz durch Laseroberflächenbehandlung von Kalt- und Warmarbeitsstählen. Germany

B.W. Morgan J.P. Thomas, 1996. A review of the development of the use of electro discharge textured and hard chromium plated work rolls within British steel strip products. Proc. of Rolls 2000 Conference., pages 176–185.

K. Spranger, K. Hilgenberg, 2019. Dispersion behavior of TiB2 particles in AISI D2 tool steel surfaces during pulsed laser dispersing and their influence on material properties. Applied Surface Science, 467-468.